NEURAL REGENERATION RESEARCH
March 2014, Volume 9, Issue 5
www.nrronline.org

rAAV/ABAD-DP-6His attenuates oxidative stress-induced injury of PC12 cells

Mingyue Jia[1], Mingyu Wang[2], Yi Yang[1], Yixin Chen[3], Dujuan Liu[4], Xu Wang[1], Lei Song[1], Jiang Wu[1], Yu Yang[1]

1 Department of Neurology, the First Hospital of Jilin University, Changchun, Jilin Province, China
2 Department of Neurology, People's Hospital of Jilin Province, Changchun, Jilin Province, China
3 Radioactive Medicine Specialty, College of Public Health in Jilin University, Changchun, Jilin Province, China
4 Department of Burn and Plastic Surgery, the General Hospital of CNPC in Jilin, Jilin, Jilin Province, China

Mingyue Jia and Mingyu Wang equally contributed to this study.

Corresponding author: *Jiang Wu, M.D., Ph.D., Department of Neurology, the First Hospital of Jilin University, Changchun 130021, Jilin Province, China, wujiang 540214@126.com. Yu Yang, M.D., Ph.D., Department of Neurology, the First Hospital of Jilin University, Changchun 130021, Jilin Province, China, yy197711@yahoo.com.cn.*

doi:*10.4103/1673-5374.130065*
http:*//www.nrronline.org/*

Accepted: *2014-02-16*

Abstract

Our previous studies have revealed that amyloid β (Aβ)-binding alcohol dehydrogenase (ABAD) decoy peptide antagonizes $A\beta_{42}$-induced neurotoxicity. However, whether it improves oxidative stress injury remains unclear. In this study, a recombinant adenovirus constitutively secreting and expressing Aβ-ABAD decoy peptide (rAAV/ABAD-DP-6His) was successfully constructed. Our results showed that rAAV/ABAD-DP-6His increased superoxide dismutase activity in hydrogen peroxide-induced oxidative stress-mediated injury of PC12 cells. Moreover, rAAV/ABAD-DP-6His decreased malondialdehyde content, intracellular Ca^{2+} concentration, and the level of reactive oxygen species. rAAV/ABAD-DP-6His maintained the stability of the mitochondrial membrane potential. In addition, the ATP level remained constant, and apoptosis was reduced. Overall, the results indicate that rAAV/ABAD-DP-6His generates the fusion peptide, Aβ-ABAD decoy peptide, which effectively protects PC12 cells from oxidative stress injury induced by hydrogen peroxide, thus exerting neuroprotective effects.

Key Words: *nerve regeneration; neurodegenerative disease; gene therapy; Alzheimer's disease; amyloid beta peptide; amyloid beta binding alcohol dehydrogenase; adeno-associated virus; hydrogen peroxide; oxidative stress; mitochondrial dysfunction; NSFC grant; neural regeneration*

Funding: *This study was supported by the National Natural Science Foundation of China for the Youth, No. 30800338, 30801211; the National Natural Science Foundation of China, No. 30872721.*

Jia MY, Wang MY, Yang Y, Chen YX, Liu DJ, Wang X, Song L, Wu J, Yang Y. rAAV/ABAD-DP-6His attenuates oxidative stress-induced injury of PC12 cells. Neural Regen Res. 2014;9(5):481-488.

Introduction

Alzheimer's disease is a predominantly late-onset neurodegenerative disease that is age-dependent, and characterized by the progressive decline of memory, cognitive functions, and changes in behavior, and personality (Selkoe, 2001; Mattson, 2004; Reddy and Beal, 2008; Wang et al., 2013). Amyloid beta (Aβ) is considered to be an important initiating molecule in the pathogenesis of Alzheimer's disease (Selkoe, 2002). Recent findings have confirmed that intraneuronal accumulation of Aβ precedes the deposition of amyloid plaques and the appearance of neurofibrillary tangles, which are consistent with the first pathological manifestation of deficits in synaptic plasticity and learning and memory (Billings et al., 2005; Wirths and Bayer, 2012). Using the yeast two-hybrid system, Yan et al. (1997) have shown that Aβ-binding alcohol dehydrogenase (ABAD) in the mitochondrial matrix is involved in multiple aspects of metabolic homeostasis as a short-chain dehydrogenase. Aβ-ABAD distorts the structure of the enzyme and modifies its functions in metabolic homeostasis related to energy metabolism and catabolism of isoleucine branched-chain fatty acids. This binding also leads to accumulation of multiple metabolic intermediates and decreases activities of the Krebs cycle and cellular respiration. These findings indicate that the effects of Aβ-ABAD may exacerbate Alzheimer's disease pathology. Therefore, blocking Aβ-ABAD-mediate effects with ABAD decoy peptide (ABAD-DP) may be a potential therapeutic strategy for Alzheimer's disease (Xie et al., 2006; Yao et al., 2011).

Oxidative stress is thought to play a major role in the etiology of Alzheimer's disease. Evidence suggests that reactive oxygen species (ROS) damage macromolecules, including lipids, proteins, and DNA (Jomova et al., 2010). Studies have also shown that the expression of oxidative stress markers is elevated in neurons surrounding Aβ deposits in transgenic mouse models of Alzheimer's disease (Pappolla et al., 1998). Aβ accumulation also occurs in primary neurons with induced oxidative stress (Goldsbury et al., 2008).

Our group has previously established a lentiviral expression system in which thioredoxin-1-ABAD-DP (TA) allows the stable expression of small ABAD-DP by fusion with cytosolic thioredoxin-1. Overexpression of TA aptamer has been shown to protect PC12 cells from intracellular Aβ cytotoxicity (Yang et al., 2007). However, whether ABAD-DP inhibits oxidative stress is unclear. In the present study, we investigated the role of recombinant adeno-associated viral

vector (rAAV) with the fusion peptide fragment, ABAD-DP-6-His protein (6His), in oxidative stress and its effect on H_2O_2-induced oxidative stress in PC12 cells. To construct ABAD-DP-6His, we fused 6His to the 5′ end of ABAD-DP cDNA in the AAV.

Materials and Methods

Cell culture

Human embryonic kidney (HEK) 293T cells and PC12 cells (Chinese Academy of Sciences, Shanghai, China) were grown in Dulbecco's modified Eagle's medium containing 10% fetal bovine serum. The cells were digested with 0.02% ethylenediaminetetraacetic acid in PBS, and maintained at 37°C under 5% CO_2 for 24–48 hours (Billings et al., 2005).

Construction of recombinant plasmid

ABAD-DP cDNA was synthesized in the plent/TRX-ABAD-DP-prepro plasmid by polymerase chain reaction (PCR) (Selkoe, 2001). The oligonucleotides (BioAsia Bioengineering Co, Shanghai, China) used were as follows: upstream primer, 5′-G CAC GTG GCA GGC ATC GCG GTG GCT AG-3′; downstream primer, 5′-G GGA TCC TCA TAC ATC AAG AAC TCG CTG G-3′. Amplifications were performed on a DNA Thermal Cycler (Sino-American, Zhengzhou, Henan Province, China) with standard PCR procedure temperatures (94°C pre-denaturation for 300 seconds, 94°C denaturation for 60 seconds, 57°C annealing for 60 seconds, 72°C extension for 70 seconds, for 30 cycles in total). ABAD-DP cDNA was assembled in a pGEM-T Easy plasmid (Promega, Madison, WI, USA), and the proper orientation was confirmed by restriction analysis using *Pma*CI and *Bam*HI (Sino-American). The integrity of the coding sequence was purified and sequenced by Sanger dideoxy sequencing (http://www.ncbi.nlm.nih.gov/genbank) (Sanger et al., 1977).

A universal recombinant rAAV vector was created, according to Smith et al. (2000). The AAV Rep and Cap genes between inverted terminal repeats of pSSV9inte plasmid were replaced by expressing the cassette from the pACCMVpLpA plasmid (Hua Guang Bioengineering Co., Xi'an, Shaanxi Province, China), which consisted of a cytomegalovirus (CMV) promoter, a multiple cloning site, and a poly A signal. The resultant new plasmid was named pSSVHG-CMV. The ABAD-DP fusion gene, obtained from the product of the plasmid, pGEM-T Easy/ABAD-DP, by the digestion with *Pma*CI and *Bam*HI, was inserted into the multiple cloning site of pSSGH/NT4-TAT-6His-prepro plasmid to generate recombinant pSSHG/ABAD-DP-6His plasmid (Figure 1A). The ABAD-DP-6His cDNA orientation was confirmed by restriction analysis using *Eco*RI and *Bam*HI.

rAAV/ABAD-DP-6His was obtained by co-transfection of pSSHG/ABAD-DP-6His with pGF140 and pAAV/Ad (Hua Guang Bioengineering Co.) in HEK293 cells (Chinese Academy of Sciences) using the calcium phosphate method (Hantschel et al., 1966). After 96 hours of transfection, the rAAV/ABAD-DP-6His viruses were harvested.

Determination of a virus titer

The titers of rAAV/ABAD-DP-6His were determined by fluorescent Real-Time PCR with SYBR Green I (Tiangen, Beijing, China). The primer contained: an upstream primer, 5′-C AAG TAC GCC CCC TAT TGA C-3′ and a downstream primer, 5′-AAG TCC CGT TGT TGA TTT TGG TG-3′. The recombinant virus was digested by Proteinase K, and the total DNA was extracted by the routing phenol-chloroform method (Reed et al., 2006). Amplifications were performed on the iQ5 Real-Time PCR Detection System (Tiangen) with the following temperature profile: 94°C for 180 seconds, 40 cycles at 94°C for 60 seconds, 54°C for 60 seconds, 68°C for 30 seconds, and extension at 72°C for 300 seconds.

Drug treatment of PC12 cells

PC12 cells were divided into four groups: (1) vehicle control, (2) 300 μmol/L H_2O_2, (3) AAV vector + 300 μmol/L H_2O_2, and (4) rAAV/ABAD-DP-6His + 300 μmol/L H_2O_2. Cells from all groups were cultured at 37°C with 5% CO_2 for 24 hours. The AAV vector + H_2O_2 and rAAV/ABAD-DP-6His + H_2O_2 groups were infected by rAAV at a multiplicity of infection of 1:100 for 24 hours. Cells were then incubated at 37°C with 5% CO_2 for 2 hours in fresh medium, and then incubated at 37°C with 5% CO_2 for additional 24 hours. The morphological changes of PC12 cells were observed by an inverted phase-contrast microscope (Olympus, Tokyo, Japan).

3-(4,5-Dimethylthiazol-2-yl)-2,5-diphenyltetrazolium bromide (MTT) assay for PC12 cells

The MTT assay was used for the determination of cell viability (Billings et al., 2005). Briefly, cells were cultured at a concentration of 5,000 cells/well in 96-well plates, at 37°C with 5% CO_2. After treatment, 20 μL MTT (5 mg/mL; Sigma-Aldrich, Los Angeles, CA, USA) was added to each well, and incubated for 4 hours at 37°C. The cell culture medium was then removed, and 100 μL of dimethyl sulfoxide was added to the wells. The plates were briefly shaken at 60 r/min for 5 minutes to dissolve the precipitates and remove the bubbles. Absorbance was read at 490 nm using the Model 550 microplate reader (Bio-Rad, Los Angeles, CA, USA).

Flow cytometry of PC12 cells for apoptosis, ROS, mitochondrial membrane potential ($\Delta\psi m$) and Ca^{2+} concentration

For the detection of apoptosis, 5 μL of Annexin V/fluorescein isothiocyanate and 10 μL of propidium iodide (20 μg/mL) (Beyotime, Beijing, China) were added to 100 μL of cell suspension. 2′,7′-Dichlorofluorescein diacetate (20 μmol/L), rhodamine123 (5 μmol/L), and acetoxymethyl ester (5 μmol/L) of Fluo-3 (Fluo-3/AM; Sigma-Aldrich) were used as fluorescent probes for the detection of ROS, $\Delta\psi m$, and Ca^{2+} concentration, respectively. Fluorescent agent (5 μL) was added to each test tube. PC12 cells were incubated for 30 minutes in the dark at 37°C, washed twice with 0.01 mol/L PBS, and centrifuged at 1,500 r/min for 5 minutes. The mean fluorescence intensity of 10,000 cells was measured for all groups using flow cytometry (BD, Los Angeles, CA, USA).

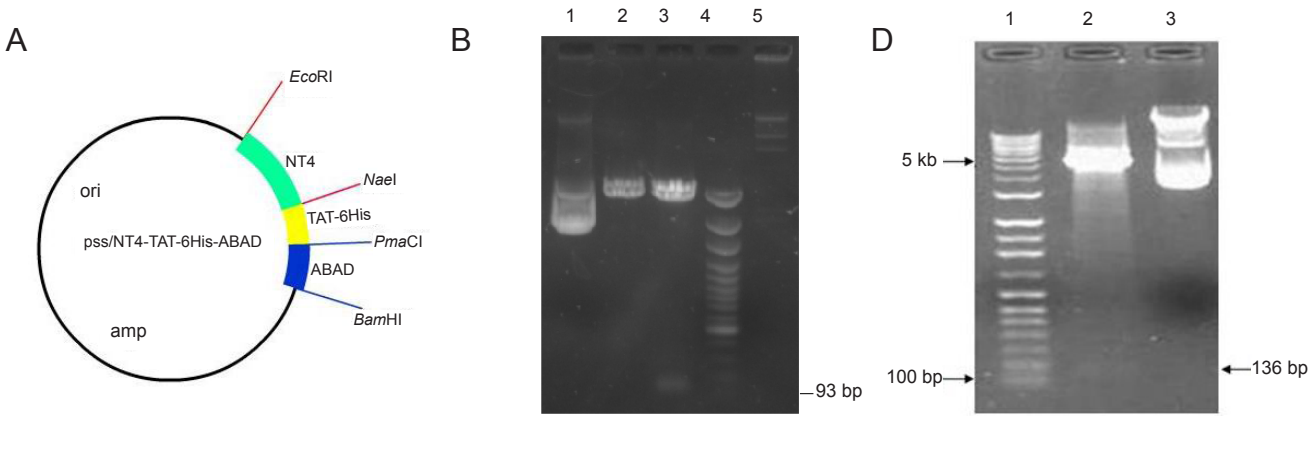

C

```
File1: H07_AA~1.SEQ
Mode: Normal                60 -     200
File2: 6HISABAD.TXT
Mode: Normal                 1 -     126
Matching Percentage (Total Window: 89%, Alignment Window: 100%)

  60 CGGGATTGGAATTCATGCATCATCATCATCATCACGTGGCAGGCATCGCG  109
     ||||||||||||||||||||||||||||||||||||||||||||||||||
  -7 ........GAATTCATGCATCATCATCATCATCACGTGGCAGGCATCGCG   42

 110 GTGGCTAGCAAGACGTACAACTTAAAGAAGGGCCAGACCCATACCTTGGA  159
     ||||||||||||||||||||||||||||||||||||||||||||||||||
  43 GTGGCTAGCAAGACGTACAACTTAAAGAAGGGCCAGACCCATACCTTGGA   92

 160 AGACTTCCAGCGAGTTCTTGATGTATGAGGATCCCAATCAC.........  209
     ||||||||||||||||||||||||||||||||||
  93 AGACTTCCAGCGAGTTCTTGATGTATGAGGATCC.................  142
```

Figure 1 Construction and identification of recombinant adenovirus helper plasmid pHelper/recombinant adenovirus/amyloid β (Aβ)-binding alcohol dehydrogenase decoy peptide-6His (pSSHG/ABAD-DP-6His) plasmid.
(A) The construction of recombinant plasmid pSSHG/ABAD-DP-6His. (B) Restriction enzyme digestion of recombinant plasmid pGEM-T Easy/ABAD-DP. Lane 1: Recombinant plasmid pGEMT-Easy/ABAD-DP; lane 2: pGEM-T Easy/ABAD-DP cut with *Eco*RI; lane 3: pGEM-T Easy/ABAD-DP cut with *Xho*I; lane 4: HBI 1.0 kb plus DNA ladder, lane 5: λDNA/*Hin*dIII marker. (C) The results of ABAD-DP-6His DNA sequencing and the comparison with our designed sequence using DNASIS software (MiraiBio, Tokyo, Japan). File 1: Gene sequencing of ABAD-DP-6His. File 2: Gene sequencing provided by GeneBank (http://www.ncbi.nlm.nih.gov/genbank). (D) Recombinant plasmid pSSHG/ABAD-DP-6His was digested with *Eco*RI and *Bam*HI and confirmed that the ABAD-DO-6his fusion gene was 136 bp, which was consistent with the expected size. Lane 1: HBI 1.0 kb plus DNA ladder; lane 2: pSSHG/ABAD-DP-6His cut with *Eco*RI and *Bam*HI. lane 3: Recombinant plasmid pSSHG/ABAD-DP-6His. ABAD: Aβ-binding alcohol dehydrogenase; DP: decoy peptide; 6His: 6-His protein.

Biochemical assays of PC12 cells

PC12 cells were seeded into 75 mm^2 petri dishes at the density of 1×10^7 cells/mm^2. After treatment with H_2O_2, cells were collected in 2-mL Eppendorf tubes, and washed three times with balanced salt solution; PC12 cells were incubated for 30 minutes in the dark at 37°C, washed twice with 0.01 mol/L PBS, centrifuged at 1,500 r/min for 10 minutes, and the supernatant was discarded. Balanced salt solution (1 mL) was added and the cells were lysed using ultrasound. The concentrations of malondialdehyde, ATP, and superoxide dismutase (SOD) were measured in the resulting homogenate using malondialdehyde test kit, ATP test kit, and SOD test kit, respectively (Nanjing Jiancheng Bioengineering Institute, Nanjing, Jiangsu Province, China). After the enzymatic reaction, the absorbance was detected using a spectrophotometer (Chengguang Corporation, Shanghai, China) at the excitation wavelengths of 532 nm, 636 nm, and 550 nm for malondialdehyde, ATP, and SOD, respectively.

Statistical analysis

All data are expressed as mean ± SD and were analyzed by one-way analysis of variance followed by the Student-Newman-Keuls test. SPSS 17.0 software (SPSS, Chicago, IL, USA) was used for statistical analysis. Significance was reached at a values of $P < 0.05$ or $P < 0.01$.

Results

Identification of recombinant plasmid and packaging of the recombinant AAV system

The ABAD-DP fusion gene was assembled in the pGEM-T Easy plasmid, and its correct orientation was confirmed by restriction analysis with *Pma*CI. A 93 bp fragment was observed by agarose gel electrophoresis (Figure 1B). The integrity of the coding sequence showed 100% consistency with the corresponding GenBank sequence (Figure 1C). The ABAD-DP cDNA was then inserted into the multiple cloning site of the pSSCMV/6His-prepro plasmid to generate the recombinant pSSHG/ABAD-DP-6His plasmid. Consistent with the theoretical value, a 100 bp gene product was observed after *Eco*RI and *Bam*HI digestion, confirming the correct orientation of the cDNA (Figure 1D).

rAAV/ABAD-DP decreased H_2O_2-induced apoptosis in PC12 cells

PC12 cells in the control group exhibited normal morphology (Figure 2A1). Oxidant treatment caused damage to these cells, with many dead neurons and debris of disintegrated cells, and neurons with markedly swollen somas (Figure 2A2, 3). H_2O_2 co-treated with rAAV/ABAD-DP-6His induced similar damage, but with most neurons maintaining somewhat normal somas, intact axons, and exuberant synapse connections.

Flow cytometry results showed that the number of apoptotic cells was significantly ($P < 0.05$) higher in the H_2O_2 group and AAV vector + H_2O_2 group compared with the control group. Furthermore, number of apoptotic cells was significantly ($P < 0.05$) lower in the rAAV/ABAD-DP-6His + H_2O_2 group compared with the H_2O_2 group (Figure 2C). However, the H_2O_2 group and the AAV vector + H_2O_2 group

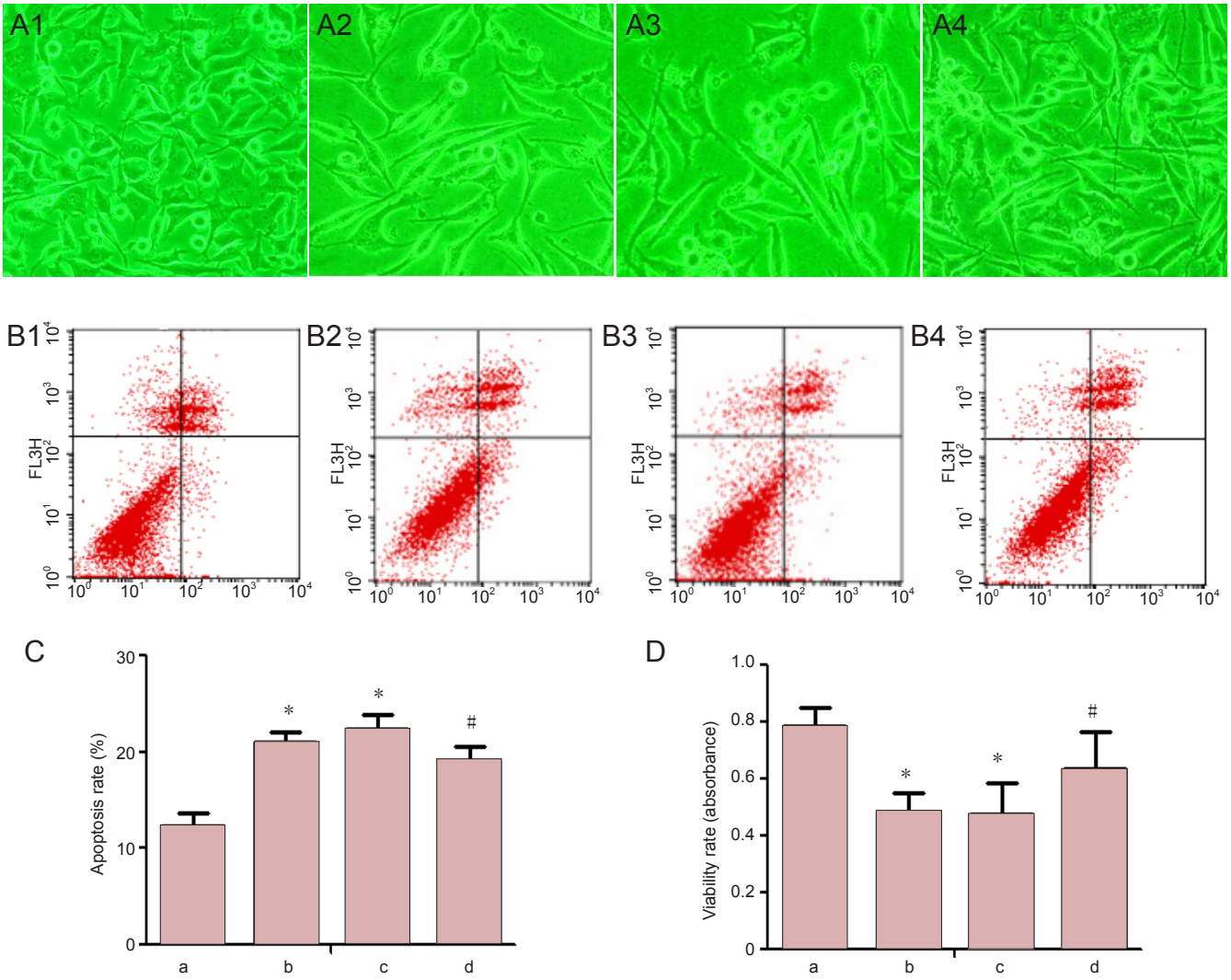

Figure 2 Protective effect of rAAV/ABAD-DP on H_2O_2-mediated changes in morphology, viability, and apoptotic activity of PC12 cells.
(A) Effect of rAAV/ABAD-DP on the morphology of PC12 cells treated with H_2O_2 (× 200). (B, C) Flow cytometry showing the effect of rAAV/ABAD-DP on H_2O_2-induced apoptosis of PC12 cells. (D) 3-(4,5-Dimethylthiazol-2-yl)-2,5-diphenyltetrazolium bromide (MTT) assay showing the effect of rAAV/ABAD-DP on H_2O_2-mediated proliferation of PC12 cells. (A1, B1, a) Normal control group; (A2, B2, b) H_2O_2 group; (A3, B3, c) AAV vector + H_2O_2 group; (A4, B4, d) rAAV/ABAD-DP-6His + H_2O_2 group. Each treatment was performed in triplicate. All data are expressed as mean ± SD and were analyzed by one-way analysis of variance followed by the Student-Newman-Keuls test. *$P < 0.05$, *vs.* normal control group; #$P < 0.05$, *vs.* H_2O_2 group. ABAD: Aβ-binding alcohol dehydrogenase; DP: decoy peptide; rAAV: recombinant adeno-associated viral vector; 6His: 6-His protein.

showed similar number of apoptotic cells (Figure 2B, C). MTT assay results indicated that cell viability in the H_2O_2 group and AAV vector + H_2O_2 group was significantly ($P < 0.05$) decreased compared with the control group. Furthermore, cell viability in the rAAV/ABAD-DP-6His + H_2O_2 group was significantly ($P < 0.05$) higher than the H_2O_2 group (Figure 2D). However, cell viability in the H_2O_2 group and AAV vector + H_2O_2 group was similar (Figure 2D).

rAAV/ABAD-DP increased the antioxidant capacity of H_2O_2-mediated damage to PC12 cells

Spectrophotometry results showed that SOD activity and ATP content were significantly ($P < 0.01$) decreased in the H_2O_2 group and rAAV/ABAD-DP-6His + H_2O_2 group compared with the control group (Figure 3A, C). Malondialdehyde content was significantly increased in the H_2O_2 group ($P < 0.05$) and rAAV/ABAD-DP-6His + H_2O_2 group ($P < 0.01$) compared with the control group (Figure 3B). Moreover, SOD activity and ATP content in the rAAV/ABAD-DP-6His + H_2O_2 group was markedly ($P < 0.01$) higher, but malondialdehyde content in this group was significantly ($P < 0.01$) lower than in the H_2O_2 group (Figure 3A–C). SOD activity, ATP content, and malondialdehyde content between the H_2O_2 group and the AAV vector + H_2O_2 group was similar (Figure 3A–C).

rAAV/ABAD-DP improved mitochondrial dysfunction in H_2O_2-mediated damage of PC12 cells

Flow cytometry results showed that the mitochondrial membrane potential was significantly reduced in the H_2O_2 group ($P < 0.05$) and rAAV/ABAD-DP-6His + H_2O_2 group

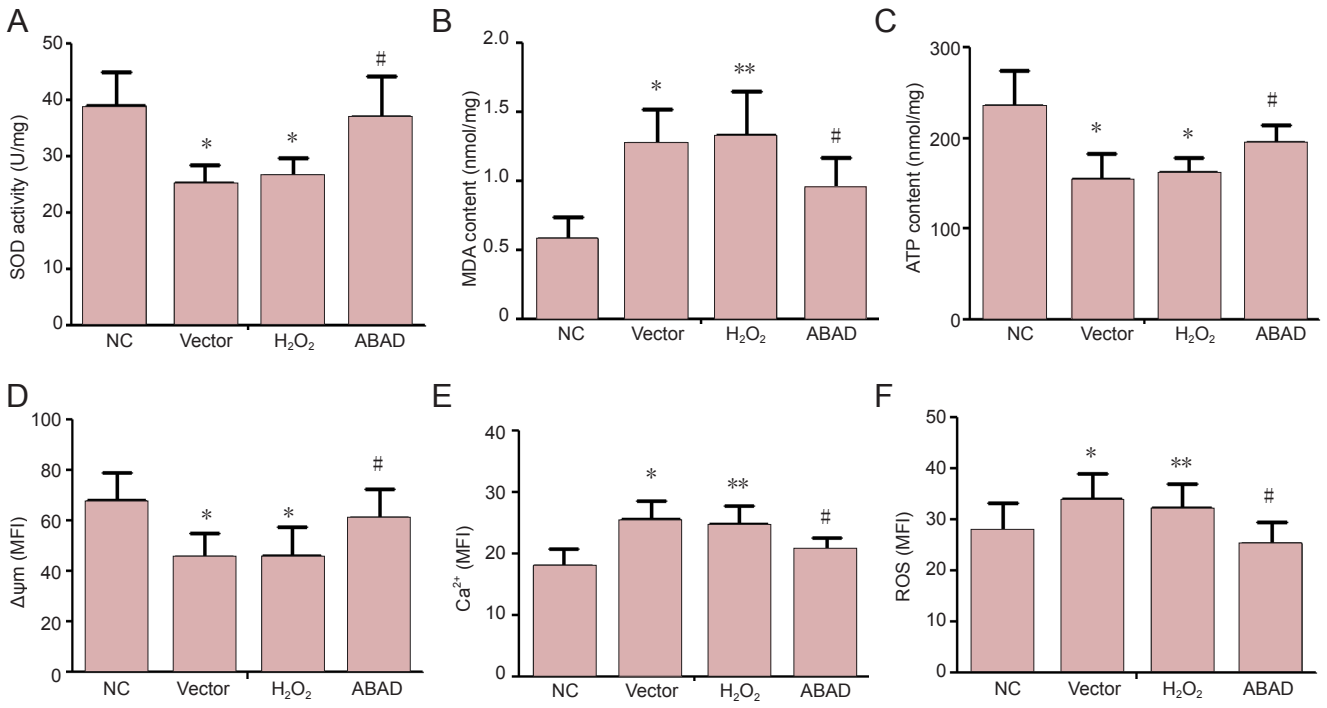

Figure 3 Protective effects of rAAV/ABAD-DP-6His with different treatments on oxidative reaction and mitochondrial dysfunction in H_2O_2-induced damage of PC12 cells.

(A) Superoxide dismutase (SOD) activity; (B) malondialdehyde (MDA) content; (C) ATP content; (D) mitochondrial membrane potential (Δψm); (E) Ca^{2+} concentration; (F) reactive oxygen species (ROS). Each treatment was performed in triplicate. All data are expressed as mean ± SD and were analyzed by one-way analysis of variance followed by the Student-Newman-Keuls test. $*P < 0.01$, $**P < 0.05$, *vs.* normal control group; $\#P < 0.01$, *vs.* H_2O_2 group. NC: Normal control group; Vector: AAV vector + H_2O_2 group; ABAD: rAAV/ABAD-DP-6His + H_2O_2 group.

($P < 0.01$) compared with the control group (Figure 3D). Ca^{2+} concentration and reactive oxygen species levels were significantly increased in the H_2O_2 group ($P < 0.05$) and rAAV/ABAD-DP-6His + H_2O_2 group ($P < 0.01$) compared with the control group (Figure 3E, F). Furthermore, ROS levels and Ca^{2+} concentration in the rAAV/ABAD-DP-6His + H_2O_2 group was significantly ($P < 0.01$) lower than those of the H_2O_2 group (Figure 3E, F); however, mitochondrial membrane potential was significantly ($P < 0.01$) higher than that of the H_2O_2 group (Figure 3D). The mitochondrial membrane potential, Ca^{2+} concentration and reactive oxygen species levels between the H_2O_2 group and the AAV vector + H_2O_2 group were similar (Figure 3D–F).

Discussion

Vector construction

Yan et al. (1997) have shown that the L_D loop of ABAD contains a unique insertion, which is presumed to be a recognition site for Aβ. A peptide encompassing this region (residues 92–120) of human ABAD (termed ABAD-DP) was tested by surface plasmon resonance for its ability to inhibit the interaction of the intact ABAD with Aβ. ABAD-DP inhibits binding of Aβ40 and Aβ42 to immobilized intact ABAD with inhibitory constants of 4.9 and 1.7 mmol/L, respectively. In contrast, a scrambled peptide with the same amino acids but reversed sequence (ABAD [120–92] or ABAD reversed peptide [RP]) is inactive (Schwarze et al., 1999; Aarts et al., 2002). These data indicate that the L_D loop of ABAD is critical for Aβ binding to ABAD. Therefore, blocking Aβ-ABAD using ABAD-DP may be a potential therapeutic strategy for AD (Xie et al., 2006; Yao et al., 2011). However, because of its short half-life and high-synthesis costs, ABAD-DP cannot be clinically administered as a therapeutic agent.

In the present study, the ABAD-DP fusion gene was successfully inserted into the multiple cloning site of pSSGH/NT4-TAT-6His-prepro plasmid to generate a recombinant pSSHG/ABAD-DP-6His plasmid. The AAV vector was co-transfected with two helper plasmids into HEK293T cells by the calcium phosphate method and was harvested at a high titer. We sought to establish a safe and highly effective method of delivering the gene construct containing ABAD-DP cDNA into PC12 cells to constitutively produce ABAD-DP *in vivo*. AAV vectors are currently among the most frequently used viral vectors for gene therapy. AAV is a small (25-nm), non-enveloped virus that packages a linear single-stranded DNA genome (Liu et al., 2014). It belongs to the family of Parvoviridae, genus Dependovirus, thus enabling effective infection in the presence of a helper virus (either an adenovirus or herpes virus). The lack of pathogenicity, persistence, and many available serotypes of the virus have increased the potential of AVV as a delivery vehicle for gene therapy (Balazs et al., 2011; Rosenberg et al., 2012; J Dismuke et al., 2013; Ploquin et al., 2013). In the present study, the 6-His gene was inserted at the 5′ end of ABAD-DP cDNA as a molecular label to follow the expression of

the ABAD-DP gene. Because of a short half-life and high synthesis costs of ABAD-DP, the constructed rAAV/ABAD-DP-6His bound to intracellular Aβ peptide in the cytoplasm, in addition to its constitutive production and expression by AVV.

Protective agent against oxidative stress

Oxidative stress is recognized as an early event in neurodegenerative diseases such as Alzheimer's disease, and plays a key role in Aβ-induced cell death (Alhebshi et al., 2013). The complex nature and genesis of oxidative damage in Alzheimer's disease is partially due to mitochondrial abnormalities that can initiate oxidative stress. Several *in vitro* studies have shown that Aβ peptide exposure causes abnormalities of mitochondrial function, as characterized by excessive mitochondrial membrane potential depolarization, aggravated calcium buffering, uncoupling of the mitochondrial respiratory chain, reduced ATP, and increased production of ROS (Cha et al., 2012; Correia et al., 2012; Prangkio et al., 2012; Sciacca et al., 2012). These alterations are evident during Aβ oligomerization and also before the appearance of Aβ plaques and neurofibrillary tangles, thus supporting the view that oxidative stress occurs early in the development of the disease (Moreira et al., 2009). Therefore, decreasing oxidative damage and repairing antioxidant defenses are important strategies to target in early Alzheimer's disease (Smith et al., 1997; Straface et al., 2005).

Lipids are the most targeted biomolecules of oxidative stress. SOD contributes to the reduction of oxidative stress and prevents lipid damage (Hosoki et al., 2012). Lipid oxidation also gives rise to a number of secondary products. These products are mainly aldehydes, which exacerbate oxidative damage (Uchida, 2000). SOD is a group of enzymes that plays a pivotal role in metabolizing superoxide radical (O_2^{-}), preempting oxidizing chain reactions that cause extensive damage, and preventing the formation of a cascade of deleterious ROS, including H_2O_2, hypochlorite, peroxynitrate, and hydroxyl radical (Miller, 2012). Hydroperoxyl radical (HO_2^{-}) is important for SOD binding to the membrane to intercept incoming superoxide. Defects in SOD that increase intracellular [O_2^{-}] cause damage to the cell envelope (Imlay and Fridovich, 1992). Because SOD catalyzes the dismutation of O_2^{-} to H_2O_2, and is localized at distinct compartments (cytosol [for SOD1], mitochondria [for SOD2], and extracellular matrix [for SOD3]), they participate in compartmentalized redox signaling (Fukai and Ushio-Fukai, 2011). Therefore, in the present study, total SODs were tested to demonstrate the damage from oxidative stress. Malondialdehyde is the principal and most studied product of polyunsaturated fatty acid peroxidation (Marnett, 1998), and is similar to ROS forming DNA adducts, which are mutagenic. Malondialdehyde can be detected in relation with lipid peroxidation and oxidative stress (Nielsen et al., 1997). Several other pathologies involving oxidative stress have been recently studied in which malondialdehyde was used as a common oxidative stress biomarker. Malondialdehyde is the principal and most studied product of polyunsaturated fatty acid peroxidation (Del Rio et al., 2005). Our data showed that SOD activity was higher in the rAAV/ABAD-DP-6His + H_2O_2 group than in the H_2O_2 group, and malondialdehyde content was higher in the H_2O_2 group than in the rAAV/ABAD-DP-6His + H_2O_2 group. Therefore, our data indicate a protective effect of rAAV/ABAD-DP-6His against H_2O_2-induced oxidative damage.

Mitochondrial ATP production is the main energy source for intracellular metabolic pathways (Schapira, 2006). Mitochondria synthesize ATP from ADP in the mitochondrial matrix by using the energy provided by the proton electrochemical gradient (Capaldi et al., 1994; Nijtmans et al., 1995; Zeviani and Di Donato, 2004). The proton gradient establishes a proton-motive force, which has two components, a pH differential and an electrical membrane potential (Campanella et al., 2009). Ca^{2+} plays an important role in the regulation of pH and electrical membrane potential. Studies have indicated that under basal conditions, total mitochondrial Ca^{2+} content is low and that cytosolic free Ca^{2+} increases in response to extrinsic agents. The latter is likely to provoke increases in intracellular Ca^{2+} concentrations (Denton and McCormack, 1980; Hansford and Castro, 1981; Crompton, 1985). The consequent activation of oxidative metabolism would then provide an increased supply of reducing equivalents to drive respiratory chain activity and ATP synthesis (Tarasov et al., 2012). The mitochondrial matrix Ca^{2+} overload can lead to enhanced generation of ROS, triggering mitochondrial permeability transition pore and cytochrome C release, and reducing equivalents to drive respiratory chain activity and ATP synthesis, which leads to apoptosis (Brookes et al., 2004). ROS, including superoxide, singlet oxygen, hydrogen peroxides, hydroxyl free radical and nitric oxide, which are mainly generated from mitochondria, play an important role in cell death (Grivennikova and Vinogradov, 2013). Accumulating evidence strongly suggests that ROS, specifically mitochondria-generated ROS, are involved in physiological signaling cascades regulating various cellular and organ functions (Afanas'ev, 2007; Valko et al., 2007; Leuner et al., 2012; Tang et al., 2013). The production of ROS by mitochondria is recognized as a crucial event in mitochondrial metabolism and oxidative stress (Akopova et al., 2014).

This study found that increasing intracellular Ca^{2+} concentrations prevented the electric membrane potential caused by H_2O_2. The consequent activation of ROS release may increase the Ca^{2+} overload thus preventing the electric membrane potential and inducing mitochondrial permeability transition pore. This response may lead to an increase in the level of ROS that can damage the respiratory chain and result in the decrease of ATP. This vicious circle results in oxidative stress and mitochondrial damage. Similarly, our results also showed enhanced ROS formation in mitochondria after oxidative damage, which was preventable by antioxidant rAAV/ABAD-DP-6His. The rAAV/ABAD-DP-6His inhibited the increase of Ca^{2+} concentration, maintained the stability of electric membrane potential, decreased ROS levels, and ensured a constant content of ATP.

Studies addressing oxidative stress will enable researchers

to better understand the mechanisms underlying Alzheimer's disease by identifying early markers of the disease. Our group has previously investigated the mechanisms and pathogenesis of Alzheimer's disease to seek new therapeutic schedules to inhibit oxidative damage and Aβ injury of Alzheimer's disease (Wang et al., 2012; Wang et al., 2013).

Conclusion

In this study, rAAV/ABAD-DP-6His induced neuroprotective effects by binding to Aβ and also protecting against oxidative stress in a non-specific manner. Therefore, these effects may be useful for developing therapeutic strategies with the aim that early treatment will slow or prevent the progression of Alzheimer's disease by targeting oxidative stress.

Acknowledgments: *We thank Liu Y and Wang ZC from Jilin University in China for providing technical support; Yang X from Jilin Univeristy for offering plent/TRX-ABAD-DP-prepro plasmid; Zhang T from University of Pittsburgh in USA for offering ITRs of pSSV9inte plasmid; and Hao YW from Xijing Hospital, the Fourth Military Medical University of Chinese PLA in China for offering pSSGH/NT4-TAT-6His-prepro plasmid.*

Author contributions: *Jia MY conducted the experiments, performed statistical analysis, analyzed experimental data, and wrote the manuscript. Yang Y and Yang Y conceived and designed the study. Wang MY provided experimental data. Chen YX and Liu DJ integrated experimental data. Wang X and Song L assisted in conducting the experiments. Wu J was in charge of funds and revised the manuscript. All authors approved the final version of the paper.*

Conflicts of interest: *None declared.*

References

Aarts M, Liu Y, Liu L, Besshoh S, Arundine M, Gurd JW, Wang YT, Salter MW, Tymianski M (2002) Treatment of ischemic brain damage by perturbing NMDA receptor-PSD-95 protein interactions. Science 298:846-850.

Afanas'ev IB (2007) Signaling functions of free radicals superoxide & nitric oxide under physiological & pathological conditions. Mol Biotechnol 37:2-4.

Akopova OV, Kolchinskaya LI, Nosar VI, Bouryi VA, Mankovska IN, Sagach VF (2014) Effect of potential-dependent potassium uptake on production of reactive oxygen species in rat brain mitochondria. Biochemistry (Mosc) 79:44-53.

Alhebshi A, Gotoh M, Suzuki I (2013) Thymoquinone protects cultured rat primary neurons against amyloid β-induced neurotoxicity. Biochem Biophys Res Commun 433:362-367.

Balazs AB, Chen J, Hong CM, Rao DS, Yang L, Baltimore D (2011) Antibody-based protection against HIV infection by vectored immunoprophylaxis. Nature 481:81-84.

Billings LM, Oddo S, Green KN, McGaugh JL, LaFerla FM (2005) Intraneuronal Aβ causes the onset of early Alzheimer's disease-related cognitive deficits in transgenic mice. Neuron 45:675-688.

Brookes PS, Yoon Y, Robotham JL, Anders MW, Sheu SS (2004) Calcium, ATP, and ROS: a mitochondrial love-hate triangle. Am J Physiol Cell Physiol 287:C817-C833.

Campanella M, Parker N, Tan C, Hall A, Duchen M (2009) IF (1): setting the pace of the F (1) F (o)-ATP synthase. Trends Biochem Sci 34:343-350.

Capaldi RA, Aggeler R, Turina P, Wilkens S (1994) Coupling between catalytic sites and the proton channel in F1F0-type ATPases. Trends Biochem Sci 19:284-289.

Cha MY, Han SH, Son SM, Hong HS, Choi YJ, Byun J, Mook-Jung I (2012) Mitochondria-specific accumulation of amyloid β induces mitochondrial dysfunction leading to apoptotic cell death. PLoS One 7:e34929.

Correia S, Santos R, Perry G, Zhu X, Moreira P, Smith M (2012) Mitochondrial importance in Alzheimer's, Huntington's and Parkinson's diseases. Adv Exp Med Biol 724:205-221.

Crompton M (1985) The regulation of mitochondrial calcium transport in heart. Curr Top Membr Transp 25:231-276.

Del Rio D, Stewart AJ, Pellegrini N (2005) A review of recent studies on malondialdehyde as toxic molecule and biological marker of oxidative stress. Nutr Metab Cardiovasc Dis 15:316-328.

Denton RM, McCormack JG (1980) On the role of the calcium transport cycle in heart and other mammalian mitochondria. FEBS Lett 119:1-8.

Fukai T, Ushio-Fukai M (2011) Superoxide dismutases: role in redox signaling, vascular function, and diseases. Antioxid Redox Signal 15:1583-1606.

Goldsbury C, Whiteman IT, Jeong EV, Lim YA (2008) Oxidative stress increases levels of endogenous amyloid-β peptides secreted from primary chick brain neurons. Aging Cell 7:771-775.

Grivennikova VG, Vinogradov AD (2013) Mitochondrial production of reactive oxygen species. Biochemistry (Mosc) 78:1490-1511.

Hansford RG, Castro F (1981) Effects of micromolar concentrations of free calcium ions on the reduction of heart mitochondrial NAD (P) by 2-oxoglutarate. Biochem J 198:525-533.

Hantschel H, Hahnefeld H, Hahnefeld E (1966) A simple method for the enrichment of virus in tissue culture fluid by adsorption on calcium phosphate. Arch Exp Veterinarmed 20:751-766.

Hosoki A, Yonekura S-I, Zhao Q-L, Wei Z-L, Takasaki I, Tabuchi Y, Wang L-L, Hasuike S, Nomura T, Tachibana A, Hashiguchi K, Yonei S, Kondo T, Zhang-Akiyama Q (2012) Mitochondria-targeted superoxide dismutase (SOD2) regulates radiation resistance and radiation stress response in HeLa cells. J Radiat Res 53:58-71.

Imlay JA, Fridovich I (1992) Suppression of oxidative envelope damage by pseudoreversion of a superoxide dismutase-deficient mutant of Escherichia coli. J Bacteriol 174:953-961.

J Dismuke D, Tenenbaum L, Jude Samulski R (2013) Biosafety of recombinant adeno-associated virus vectors. Curr Gene Ther 13:434-452.

Jomova K, Vondrakova D, Lawson M, Valko M (2010) Metals, oxidative stress and neurodegenerative disorders. Mol Cell Biochem 345:91-104.

Leuner K, Schütt T, Kurz C, Eckert SH, Schiller C, Occhipinti A, Mai S, Jendrach M, Eckert GP, Kruse SE, Palmiter RD, Brandt U, Dröse S, Wittig I, Willem M, Haass C, Reichert AS, Müller WE (2012) Mitochondrion-derived reactive oxygen species lead to enhanced amyloid beta formation. Antioxid Redox Signal 16:1421-1433.

Liu Y, Keefe K, Tang X, Lin S, Smith GM (2014) Use of self-complementary adeno-associated virus serotype 2 as a tracer for labeling axons: implications for axon regeneration. PLoS One 9:e87447.

Marnett LJ (1998) Chemistry and biology of DNA damage by malondialdehyde. IARC Sci Publ:17-27.

Mattson MP (2004) Pathways towards and away from Alzheimer's disease. Nature 430:631-639.

Miller AF (2012) Superoxide dismutases: ancient enzymes and new insights. FEBS Lett 586:585-595.

Moreira PI, Duarte AI, Santos MS, Rego AC, Oliveira CR (2009) An integrative view of the role of oxidative stress, mitochondria and insulin in Alzheimer's disease. J Alzheimers Dis 16:741-761.

Nielsen F, Mikkelsen BB, Nielsen JB, Andersen HR, Grandjean P (1997) Plasma malondialdehyde as biomarker for oxidative stress: reference interval and effects of life-style factors. Clin Chem 43:1209-1214.

Nijtmans LG, Klement P, Houštěk J, van den Bogert C (1995) Assembly of mitochondrial ATP synthase in cultured human cells: implications for mitochondrial diseases. Biochim Biophys Acta 1272:190-198.

Pappolla M, Chyan Y, Omar R, Hsiao K, Perry G, Smith M, Bozner P (1998) Evidence of oxidative stress and in vivo neurotoxicity of beta-amyloid in a transgenic mouse model of Alzheimer's disease: a chronic oxidative paradigm for testing antioxidant therapies in vivo. Am J Pathol 152:871-877.

Ploquin A, Szécsi J, Mathieu C, Guillaume V, Barateau V, Ong KC, Wong KT, Cosset FL, Horvat B, Salvetti A (2013) Protection against henipavirus infection by use of recombinant adeno-associated virus–vector vaccines. J Infect Dis 207:469-478.

Prangkio P, Yusko EC, Sept D, Yang J, Mayer M (2012) Multivariate analyses of amyloid-beta oligomer populations indicate a connection between pore formation and cytotoxicity. PLoS One 7:e47261.

Reddy PH, Beal MF (2008) Amyloid beta, mitochondrial dysfunction and synaptic damage: implications for cognitive decline in aging and Alzheimer's disease. Trends Mol Med 14:45-53.

Reed SE, Staley EM, Mayginnes JP, Pintel DJ, Tullis GE (2006) Transfection of mammalian cells using linear polyethylenimine is a simple and effective means of producing recombinant adeno-associated virus vectors. J Virol Methods 138:85-98.

Rosenberg JB, Hicks MJ, De BP, Pagovich O, Frenk E, Janda KD, Wee S, Koob GF, Hackett NR, Kaminsky SM, Worgall S, Tignor N, Mezey J, Crystal R (2012) AAVrh. 10-mediated expression of an anti-cocaine antibody mediates persistent passive immunization that suppresses cocaine-induced behavior. Hum Gene Ther 23:451-459.

Sanger F, Nicklen S, Coulson AR (1977) DNA sequencing with chain-terminating inhibitors. Proc Natl Acad Sci U S A 74:5463-5467.

Schapira AH (2006) Mitochondrial disease. Lancet 368:70-82.

Schwarze SR, Ho A, Vocero-Akbani A, Dowdy SF (1999) In vivo protein transduction: delivery of a biologically active protein into the mouse. Science 285:1569-1572.

Sciacca Michele FM, Kotler Samuel A, Brender Jeffrey R, Chen J, Lee D-k, Ramamoorthy A (2012) Two-step mechanism of membrane disruption by Aβ through membrane fragmentation and pore formation. Biophys J 103:702-710.

Selkoe DJ (2001) Alzheimer's disease: genes, proteins, and therapy. Physiol Rev 81:741-766.

Selkoe DJ (2002) Alzheimer's disease is a synaptic failure. Science 298:789-791.

Smith MA, Harris PLR, Sayre LM, Beckman JS, Perry G (1997) Widespread peroxynitrite-mediated damage in Alzheimer's disease. J Neurosci 17:2653-2657.

Smith MA, Rottkamp CA, Nunomura A, Raina AK, Perry G (2000) Oxidative stress in Alzheimer's disease. Biochim Biophys Acta 1502:139-144.

Straface E, Matarrese P, Gambardella L, Vona R, Sgadari A, Silveri MC, Malorni W (2005) Oxidative imbalance and cathepsin D changes as peripheral blood biomarkers of Alzheimer disease: a pilot study. FEBS Lett 579:2759-2766.

Tang DW, Fang Y, Liu ZX, Wu Y, Wang XL, Zhao S, Han GC, Zeng SM (2013) The disturbances of endoplasmic reticulum calcium homeostasis caused by increased intracellular reactive oxygen species contributes to fragmentation in aged porcine oocytes. Biol Reprod 89:124.

Tarasov AI, Griffiths EJ, Rutter GA (2012) Regulation of ATP production by mitochondrial Ca(2+). Cell Calcium 52:28-35.

Uchida K (2000) Role of reactive aldehyde in cardiovascular diseases. Free Radic Biol Med 28:1685-1696.

Valko M, Leibfritz D, Moncol J, Cronin MT, Mazur M, Telser J (2007) Free radicals and antioxidants in normal physiological functions and human disease. Int J Biochem Cell Biol 39:44-84.

Wang MY, Yang Y, Wu J, Wang X, Che LH, Sun X, Yang Y (2012) Construction of recombinant adeno-associated virus system secreting expression of ABAD-DP. Zhongfeng yu Shenjing Jibing Zazhi 29:292-296.

Wang W, Zhang HT, Wang SH, Zhang YB (2013) Correlation of Alzheimer's disease with Wnt signaling pathway and neural stem cells. Zhongguo Zuzhi Gongcheng Yanjiu 17:3566-3572.

Wang X, Yang Y, Jia MY, Ma C, Wang MY, Che LH, Yang Y, Wu J (2013) The novel amyloid-beta peptide aptamer inhibits intracellular amyloid-beta peptide toxicity. Neural Regen Res 8:39-48.

Wirths O, Bayer TA (2012) Intraneuronal Aβ accumulation and neurodegeneration: lessons from transgenic models. Life Sci 91:1148-1152.

Xie Y, Deng S, Chen Z, Yan S, Landry DW (2006) Identification of small-molecule inhibitors of the Aβ–ABAD interaction. Bioorg Med Chem Lett 16:4657-4660.

Yan SD, Fu J, Soto C, Chen X, Zhu H, Al-Mohanna F, Collison K, Zhu A, Stern E, Saido T, Tohyama M, Ogawa S, Roher A, Stern D (1997) An intracellular protein that binds amyloid-β peptide and mediates neurotoxicity in Alzheimer's disease. Nature 389:689-695.

Yang X, Yang Y, Wu J, Zhu J (2007) Stable expression of a novel fusion peptide of thioredoxin-1 and ABAD-inhibiting peptide protects PC12 cells from intracellular amyloid-beta. J Mol Neurosci 33:180-188.

Yao J, Du H, Yan S, Fang F, Wang C, Lue LF, Guo L, Chen D, Stern DM, Gunn Moore FJ, Xi Chen J, Arancio O, Yan S (2011) Inhibition of amyloid-β (Aβ) peptide-binding alcohol dehydrogenase-Aβ interaction reduces Aβ accumulation and improves mitochondrial function in a mouse model of Alzheimer's disease. J Neurosci 31:2313-2320.

Zeviani M, Di Donato S (2004) Mitochondrial disorders. Brain 127: 2153-2172.

Copyedited by Mark F, Robens J, Yu J, Yang Y, Li CH, Song LP, Zhao M